

# Degradation of oxidative stress-induced denatured albumin in rat liver endothelial cells

Ryuji Bito, Sayaka Hino, Atsushi Baba, Miharuru Tanaka, Haruka Watabe and Hiroaki Kawabata

*Am J Physiol Cell Physiol* 289:531-542, 2005. First published May 4, 2005;  
doi:10.1152/ajpcell.00431.2004

## You might find this additional information useful...

---

This article cites 58 articles, 29 of which you can access free at:

<http://ajpcell.physiology.org/cgi/content/full/289/3/C531#BIBL>

This article has been cited by 4 other HighWire hosted articles:

**Age-related changes in the expression and oxidation of bronchoalveolar lavage proteins in the rat**

T. M. Umstead, W. M. Freeman, V. M. Chinchilli and D. S. Phelps

*Am J Physiol Lung Cell Mol Physiol*, January 1, 2009; 296 (1): L14-L29.

[Abstract] [Full Text] [PDF]

**Canalicular Mrp2 localization is reversibly regulated by the intracellular redox status**

S. Sekine, K. Ito and T. Horie

*Am J Physiol Gastrointest Liver Physiol*, November 1, 2008; 295 (5): G1035-G1041.

[Abstract] [Full Text] [PDF]

**Disposition of Protein-bound 3-nitrotyrosine in Rat Plasma Analysed by a Novel Protocol for HPLC-ECD**

Y. H. Hitomi, J. Okuda, H. Nishino, Y. Kambayashi, Y. Hibino, K. Takemoto, T. Takigawa, H. Ohno, N. Taniguchi and K. Ogino

*J. Biochem.*, April 1, 2007; 141 (4): 495-502.

[Abstract] [Full Text] [PDF]

**Clathrin-mediated endocytosis of FITC-albumin in alveolar type II epithelial cell line RLE-6TN**

R. Yumoto, H. Nishikawa, M. Okamoto, H. Katayama, J. Nagai and M. Takano

*Am J Physiol Lung Cell Mol Physiol*, May 1, 2006; 290 (5): L946-L955.

[Abstract] [Full Text] [PDF]

Updated information and services including high-resolution figures, can be found at:

<http://ajpcell.physiology.org/cgi/content/full/289/3/C531>

Additional material and information about *AJP - Cell Physiology* can be found at:

<http://www.the-aps.org/publications/ajpcell>

---

This information is current as of November 9, 2009 .

## Degradation of oxidative stress-induced denatured albumin in rat liver endothelial cells

Ryuji Bito, Sayaka Hino, Atsushi Baba, Miharuru Tanaka, Haruka Watabe, and Hiroaki Kawabata

Laboratory for Nutritional Biochemistry, School of Agriculture, Meiji University, Kanagawa, Japan

Submitted 31 August 2004; accepted in final form 20 April 2005

**Bito, Ryuji, Sayaka Hino, Atsushi Baba, Miharuru Tanaka, Haruka Watabe, and Hiroaki Kawabata.** Degradation of oxidative stress-induced denatured albumin in rat liver endothelial cells. *Am J Physiol Cell Physiol* 289: C531–C542, 2005. First published May 4, 2005; doi:10.1152/ajpcell.00431.2004.—We previously identified conformationally denatured albumin (D2 and D3 albumin) in rats with endotoxemia (Bito R, Shikano T, and Kawabata H. *Biochim Biophys Acta* 1646: 100–111, 2003). In the present study, we attempted first to confirm whether the denatured albumins generally increase in conditions of oxidative stress and second to characterize the degradative process of the denatured albumin using primary cultured rat liver endothelial cells. We used five models of oxidative stress, including endotoxemia, ischemic heart disease, diabetes, acute inflammation, and aging, and found that serum concentrations of D3 albumin correlate with the serum levels of thiobarbituric acid-reactive substance ( $R = 0.87$ ), whereas the concentrations of D2 albumin are 0.52. Ligand blot analysis showed that the D3 albumin binds to gp18 and gp30, which are known endothelial scavenger receptors for chemically denatured albumin. Primary cultured rat liver endothelial cells degraded the FITC-D3 albumin, and the degradation rate decreased to ~60% of control levels in response to anti-gp18 and anti-gp30 antibodies, respectively. An equimolar mixture of these antibodies produced an additive inhibitory effect on both uptake and degradation, resulting in levels ~20% those of the control. Furthermore, filipin and digitonin, inhibitors of the caveolae-related endocytic pathway, reduced the FITC-D3 albumin uptake and degradation to <20%. Laser-scanning confocal microscopic observation supported these data regarding the uptake and degradation of D3 albumin. These results indicate that conformationally denatured D3 albumin occurs generally under oxidative stress and is degraded primarily via gp18- and gp30-mediated and caveolae-related endocytosis in liver endothelial cells.

serum albumin; denaturation; scavenger receptor; caveolae

EARLY IN VIVO STUDIES with radioisotope-labeled albumin have revealed the constant plasma half-life to be 2–2.5 days in rats (41). Conformationally altered albumin, however, is well known to show an extremely short half-life in circulating blood (31). Such changes in the degradation rate of serum albumin as well as of other serum proteins seem to occur under an individual degradative process, but the underlying mechanisms have not been clarified on a molecular basis. On the other hand, experimental data show that free radical species are responsible for conformational changes and fragmentation of protein molecules (12). Again, the elimination mechanisms for these denatured proteins from circulating blood and their degradative processes in the body remain unclear.

Address for reprint requests and other correspondence: H. Kawabata, Laboratory for Nutritional Biochemistry, School of Agriculture, Meiji Univ., 1-1-1 Higashi-mita, Tama-ku, Kawasaki City, Kanagawa 214-8571, Japan (e-mail: kawabata@isc.meiji.ac.jp).

Recently, several types of receptors that bind to modified albumin have been reported. These receptors include the following: gp18 and gp30, scavenger receptors for chemically modified albumin (47, 51); LOX-1, a lectin-like oxidized low-density lipoprotein receptor 1 (23); SREC, a scavenger receptor expressed by endothelial cells for modified LDL (1); FEEL-1 and FEEL-2 (also known as stabilin-1 or stabilin-2), endocytic receptors for advanced glycation end product (AGE) (20, 55); SR-A, a scavenger receptor class A for modified LDL (27, 28); RAGE, a receptor for AGE (33); OST-48, a 48-kDa member of the oligosaccharyltransferase complex; 80K-H, an 80- to 87-kDa protein substrate for protein kinase C (29); and unnamed 15-, 35-, and 85-kDa proteins (38, 39, 44). Among these binding proteins, gp18 and gp30 were originally reported by Schnitzer and colleagues (47, 51), who characterized the binding properties between the membrane protein fraction from endothelial cells and chemically modified albumins such as maleylated and formylated albumin. They also showed that gp18- and gp30-mediated endocytosis is one route for the degradation of chemically denatured albumin.

In addition to the cell surface receptors that recognize the modified albumin, intracellular events leading to lysosomal degradation have also been investigated. Caveolin is an intracellular protein that participates in the transportation of molecules inside cells. Caveolin-coated plasmalemmal vesicles (caveolae) have been found to transport many molecules, including lipids, acylated proteins, membrane receptors and transporters, structural molecules, and so forth (6, 45). Chemically modified albumins such as maleylated and formylated albumins also have been reported to transport by the caveolae-mediated endocytosis leading to the lysosome (46, 50).

Although the findings summarized above are thought to provide important evidence regarding the degradative mechanisms of denatured albumin in the body, all of these results were obtained using chemically, that is, artificially, modified albumins. As such, it remains unclear whether the denatured albumin generated in the body behaves in the same way as the chemically modified albumins. We recently isolated and characterized denatured albumin (D2 and D3 albumin) from rats with endotoxemia (4). In the present study, we first attempted to clarify whether the physiologically denatured albumins (D2 and D3 albumin) are generally produced by oxidative stress in the body. Next, using the physiologically denatured albumin and primary cultured liver endothelial cells (LECs), we attempted to clarify 1) whether physiologically denatured albumin binds to gp18 and gp30 cell surface receptors that have been confirmed using chemically modified albumins, 2) whether physiologically denatured albumin reaches the lyso-

The costs of publication of this article were defrayed in part by the payment of page charges. The article must therefore be hereby marked “advertisement” in accordance with 18 U.S.C. Section 1734 solely to indicate this fact.

some via caveolae-mediated endocytosis after attaching to cell surface receptors gp18 and gp30, and 3) the relative contribution of gp18- and gp30-mediated endocytosis to the breakdown of physiologically denatured albumin in endothelial cells.

## MATERIALS AND METHODS

### Materials

*N*<sup>o</sup>-nitro-L-arginine methyl ester (L-NAME), streptozotocin (STZ), fluorescein isothiocyanate (FITC), lipopolysaccharide (LPS; serotype type L-4130), fluoresceinamin, filipin, phenyl arsine oxide (PAO), and fucoidan were purchased from Sigma Chemical (St. Louis, MO). Blue Sepharose CL-6B, Sephacryl S-300, DEAE Sephadex A-50, Cy3 fluorescent dye, and cyanogen bromide-activated Sepharose CL4B were obtained from Amersham Biosciences (Piscataway, NJ). Alexa Fluor 488 and LysoTracker Red DND-99 were purchased from Molecular Probes (Eugene, OR). FITC-labeled anti-rabbit IgG (goat) was obtained from Vector Laboratories (Burlingame, CA). 2,4,6-trinitrobenzenesulfonic acid (TNBS) was purchased from Kanto Kagaku (Tokyo, Japan). Sodium dextran sulfate was obtained from MP Biomedicals (Aurora, OH). Concanavalin A and collagenase were purchased from Wako Pure Chemical Industries (Osaka, Japan). All other chemicals used were of analytical grade.

### Experiment 1: Induction of Oxidative Stress and Determination of Denatured Albumin

**Animals.** Male Wistar rats (6 wk and 6 mo old) were purchased from Japan Laboratory Animals (Tokyo, Japan). The rats were housed in a light-cycle room lit from 8 AM to 8 PM at a temperature of 22°C, and the animals were allowed free access to commercial chow and water for 1 wk.

Young rats (6 wk old) were orally administered NO synthase inhibitor L-NAME in drinking water (1 mg/ml; Ref. 25) to induce ischemic heart disease (IHD). Their daily intake of L-NAME was from 25 to 40 mg/day. Diabetes was induced by administering an intraperitoneal injection of STZ (65 mg/kg body wt; Ref. 40). The plasma levels of glucose were  $468 \pm 29$  mg/dl at 7 days after the STZ injection. Acute inflammation was induced by a subcutaneous injection of turpentine oil (5 ml/kg body wt; Ref. 52). Endotoxemia was induced by administering an intraperitoneal injection of LPS (5 mg/kg body wt; Ref. 4). These rats with induced IHD, diabetes, acute inflammation, and endotoxemia were killed by performing thoracic incisions after withdrawal of the blood samples while the rats were under Nembutal anesthesia at 1.5, 2, 7, and 10 days after the respective operations. Six-month-old rats were killed without having undergone any operation for comparison with the age-related changes with 6-wk-old rats. Plasma thiobarbituric acid-reactive substance (TBARS) was determined fluorometrically using the method of Yagi (59).

All procedures concerning the animal experiments were performed according to the guidelines established by the Institutional Animal Care and Use Committee of Meiji University.

**Preparation of native, chemically modified, and physiologically denatured albumin.** Rat serum albumin was purified according to a previously described method (4). Briefly, after being dialyzed against 50 mM Tris·HCl buffer (pH 7.0) containing 50 mM sodium chloride, rat plasma was applied to a Blue Sepharose CL-6B and Sephacryl S-300 column. Serum albumin eluted in the major peak of the gel chromatography was used as "native albumin" ( $\alpha$ -helix content was >67%; Ref. 9). The purity of the albumin was confirmed by performing SDS-PAGE.

Two kinds of chemically modified albumins, formylated albumin (F-Alb) and maleylated albumin (M-Alb), were prepared. 1) Formylation of albumin was performed according to a previously described method (21). The purified native albumin (8 ml of 4 mg/ml native albumin) was mixed with formaldehyde solution (final concentration

20% vol/vol) and incubated for 1 h at 37°C and then dialyzed against phosphate-buffered saline (PBS). 2) Maleylation of albumin was performed according to a previously described method (7). After being dialyzed against 0.1 M sodium pyrophosphate buffer (pH 9.0), the purified native albumin (5 ml of 4 mg/ml) was mixed with 0.5 ml of 1 M maleic anhydride in 1,4-dioxane at pH 9.0 and left for 5 min at 2°C and then dialyzed against PBS. Free amino groups of each albumin were determined using the TNBS method (17). The formylation and maleylation of the amino groups of the albumin molecule occurred at 37.7 and 95.5% efficiency, respectively. The  $\alpha$ -helix contents for F-Alb and M-Alb were 32.4 and 31.4%, respectively.

D2 and D3 albumins were isolated according to a previously described method (4). The Blue Sepharose CL-6B, Sephacryl S-300, and DEAE Sephadex A-50 columns were used to isolate these albumins from rats that had received five kinds of oxidative stress (IHD, diabetes, acute inflammation, endotoxemia, and aging). The conformational nature of these albumins was confirmed using CD and proteolytic susceptibility analysis. Protein concentrations were determined according to the method of Bradford.

**Preparation of antibodies.** Japanese White male rabbits were immunized with native albumin or M-Alb. Freund's complete adjuvant was used for the first immunization, and incomplete adjuvant was used for the subsequent immunizations.

The IgG against the specific epitopes of M-Alb was prepared using a previously described method (4). Briefly, anti-M-Alb IgG was mixed with an excessive amount of native albumin and left for 1 day. IgG native albumin complex was removed by performing centrifugation at 12,000 g for 20 min. The supernatant was then applied to a Blue Sepharose CL-6B column to remove free native albumin. The protein solution passing through the column was used as specific M-Alb IgG. The binding specificities of the specific M-Alb IgG against whole plasma proteins were confirmed using Western blot analysis and peptide mass fingerprinting (4).

**Quantification of total and denatured albumins.** Plasma total albumin (native + denatured forms) and denatured (D2 and D3) albumins were quantified according to a previously described method (4). Briefly, rat plasma was subjected to SDS-PAGE (for total albumin) or native PAGE (for denatured albumins). The proteins were transferred onto a polyvinylidene difluoride (PVDF) membrane at 50 V for 2 h. Total albumin was quantified using anti-native albumin antiserum (first antibody), and denatured albumins were quantified using the purified IgG against the specific epitopes of M-Alb (first antibody). The fluorescence intensity of FITC-labeled anti-rabbit goat IgG (secondary antibody) was determined using a FluorImager 595 (Amersham Biosciences, Piscataway, NJ).

**CD measurements.** CD measurements were performed according to the method of Khan et al. (26). All measurements were performed at 25°C using a spectropolarimeter (J-805; Jasco, Tokyo, Japan). Far UV CD spectra (200–250 nm) were obtained using a 0.1-cm path length cell at a protein concentration of 1.8  $\mu$ M in sodium phosphate buffer (pH 7.0). The results are expressed as the mean residue ellipticity (MRE). The helical content of the proteins was calculated using the method of Chen et al. (11).

**Proteolytic susceptibility.** The lysosomal fraction from rat liver was purified according to the method of Ohshita et al. (37). The proteolytic susceptibility of conformationally different albumins was evaluated according to a previously described method (36). These albumins were dialyzed against ultrapure water. Each protein (34  $\mu$ l of 0.4 mg/ml) was digested with 34  $\mu$ l of lysosomal enzymes (1.0 mg/ml) for 2 h at 37°C, pH 5.0. The proteolytic reaction was terminated by mixing with 32  $\mu$ l of denaturation buffer (3% SDS, 1.2% 2-mercaptoethanol, 2 M urea, 3 mM EDTA, and 0.17 M Tris·HCl, pH 7.8) and boiling for 10 min, and then the mixture was subjected to SDS-PAGE, followed by Western blot analysis. The fluorescence intensities of the original bands were determined using the FluorImager 595.

### Experiment 2: Albumin Uptake and Degradation in Primary Cultured Liver Endothelial Cells

**Protein labeling with fluorescent dyes.** FITC, Alexa 488, and Cy3 fluorescent dyes were used for protein labeling. Labeling procedures were performed according to the manufacturer's instructions. Proteins used in this part of the experiments were prepared as follows. Native albumin was purified from nontreated rats in the manner described in *Preparation of native, chemically modified, physiologically denatured (D2 and D3) albumin*. D3 albumin was isolated from rats with endotoxemia. Anti-gp18 and anti-gp30 antibodies were prepared in the manner described in *Isolation and immunization of gp18 and gp30*. Our preliminary experiments indicated that labeling with fluorescent dyes FITC and Alexa 488 had no serious influence on the conformational nature of native albumin in terms of the  $\alpha$ -helical content.

**Preparation of rat liver membrane proteins.** The membrane protein fraction from rat liver was prepared using the differential centrifugation method (39, 56). Briefly, rat liver was perfused from the hepatic portal vein using 100 ml of PBS and homogenized in 200 ml of 150 mM NaCl dissolved in *buffer A* (0.1 mM EDTA, 0.2% 2-mercaptoethanol, and 50 mM Tris·HCl, pH 8.0). After centrifugation at 105,000 g for 1 h at 4°C, the pellet was resuspended in 200 ml of *buffer B* (50 mM NaCl and 40 mM *n*-octyl- $\beta$ -D-glucopyranoside dissolved in *buffer A*). The resuspended solution was centrifuged at 105,000 g for 1 h at 4°C, and the supernatant was collected as membrane proteins.

**Isolation and immunization of gp18 and gp30.** An M-Alb affinity column was prepared according to a previously described method (28, 48). Briefly, the Sepharose 4B beads (1.5 g) were incubated at 4°C for 24 h with 45 mg of M-Alb in 50 ml of coupling buffer (0.5 M NaCl and 0.1 M NaHCO<sub>3</sub>, pH 8.3). The coupling efficiency was 1.5 mg of M-Alb/ml of gel. A membrane fraction from rat liver (2 mg of protein) was applied to the M-Alb affinity column (1 × 5 cm), and proteins were eluted from the column using the stepwise concentration of NaCl (50, 250, and 1,000 mM). These procedures were performed according to a previously described method (2, 48, 56). After confirming the positions of gp18 and gp30 on the PVDF membrane using ligand blot analysis (see below), gel pieces containing gp18 or gp30 were excised from the PAGE gels, and each protein was eluted using an electroelution apparatus (422 Electroeluter; Bio-Rad). Anti-gp18 and anti-gp30 antibody were prepared in the manner described in *Preparation of antibodies*. The binding specificities of anti-gp18 and anti-gp30 IgG against total liver membrane proteins were confirmed by SDS-PAGE followed by Western blot analysis.

**Ligand blot.** The ligand blot was performed according to the method of Schnitzer et al. (51) and our preliminary experiments using both FITC-labeled F-Alb and M-Alb. Membrane proteins (500  $\mu$ g) were separated by performing SDS-PAGE and transferred onto PVDF membrane filters at 50 V for 30 min. After being washed with PBS containing 0.1% Tween 20 (vol/vol), the filter membranes were incubated with FITC-labeled D3 albumin (30  $\mu$ g/ml) or FITC-labeled native albumin (0.03 or 3 mg/ml) for 1 h. For competition analysis with another protein, the FITC-labeled D3 albumin was mixed with unlabeled competitors (10-fold molar excess of protein competitor or 1 mg/ml of polyanionic molecules and concanavalin A; Ref. 47). Fluorescence scavenging, quenching, and insolubilization caused by the addition of nonlabeled albumins were confirmed to be negligible in our preliminary experiments.

**Isolation and culture of LECs.** LECs were separated from hepatocytes by differential centrifugation (60). Aliquots (1.3 ml) of the LEC suspensions were seeded in collagen-coated 35-mm dishes (4 × 10<sup>6</sup> cells). These LECs were incubated for 3 h at 37°C in a humidified incubator under 5% CO<sub>2</sub> in air. Each dish was washed twice with *medium A* (Williams's medium E supplemented with 10% FBS, 100  $\mu$ g/ml streptomycin, 20 mM HEPES, and 100 IU/ml penicillin) to remove nonadherent cells, after which incubation was continued for

2 h at 37°C with *medium A* excluding FBS. LEC populations in cultured cells were confirmed by confocal microscopic observation after the incorporation of fluoresceinamin-labeled ovalbumin (3  $\mu$ g/ml medium; Refs. 5, 47). The purity of the isolated LECs was 86 ± 4%.

**Binding, uptake, and degradation assay of FITC-labeled albumin.** The binding and uptake assay was performed as described previously (35). The LECs in culture were washed with *medium A* and refurnished with 1.3 ml of *medium A* containing the FITC-labeled D3 albumin with or without an excess of unlabeled ligand. After incubation for 2 h at 4°C (for the binding assay) or 37°C (for the uptake assay), the culture medium was taken from each dish. The nonspecific fluorescence was determined in the presence of unlabeled D3 albumin (a 20-fold molar excess). For the competition analysis, FITC-labeled D3 albumin was mixed with an unlabeled competitor (10-fold molar excess) or 1 mg/ml of polyanionic molecules (47) before incubation. To determine the endocytic pathway of D3 albumin, FITC-labeled D3 albumin was used for quantitative analyses, and Alexa 488-labeled D3 albumin was used for confocal microscopic observations. Filipin (5  $\mu$ g/ml) (50) and digitonin (4  $\mu$ M) (43), inhibitors of caveolae-related endocytosis, and PAO (2  $\mu$ M) (3), an inhibitor of clathrin-related endocytosis, were added to the culture medium in both the uptake and degradation assays. These dishes were washed twice using 0.35 ml of PBS, and LECs in each dish were scraped twice using 1.0 ml of homogenate buffer (4.77 g/l HEPES and 85.6 g/l sucrose, pH 7.5). Two milliliters of harvested samples were homogenized using the Polytron (PT1200; Kinematica, Lucerne, Switzerland) and then centrifuged at 8,000 g for 10 min at 4°C. The supernatant was transferred to microplates, the fluorescence intensity was determined using the FluorImager 595, and cellular protein was estimated using the method described above.

To quantify the degradation of FITC-labeled albumin, the intensity of TCA-soluble fluorescence was measured according to the method of Gekle et al. (18). Briefly, LECs were cultured with FITC-labeled D3 albumin in the manner described in *Isolation and culture of LECs*. After a 2-h incubation, cells were harvested and homogenized in the manner described above. One milliliter of 10% TCA was added to 1 ml of cellular homogenate and kept in an ice-cold bath for 10 min. After centrifugation at 8,000 g for 10 min, the supernatant was adjusted to pH 7.4 using a 1 M Na<sub>2</sub>HPO<sub>4</sub> buffer. The fluorescence of the supernatant was determined using the FluorImager 595.

**Confocal microscopy.** Confocal images were captured according to the method of John et al. (22). Briefly, glass-bottomed culture dishes (MatTek, Ashland, MA) were coated with collagen using 0.03% collagen in 0.1 N acetic acid. LECs were cultured for 2 h with *medium A* containing the following fluorescent probes: 1) LysoTracker (50 nM) and Alexa 488-labeled D3 albumin (2  $\mu$ g/ml), 2) Cy3-labeled anti-gp18 IgG (3  $\mu$ g/ml) and Alexa 488-labeled D3 albumin (20  $\mu$ g/ml), and 3) LysoTracker (50 nM) and Alexa 488-labeled D3 albumin (2  $\mu$ g/ml) with unlabeled anti-gp18 and anti-gp30 IgG (50  $\mu$ g/ml each). Confocal images of LECs were captured using a laser-scanning confocal microscope (LSM 510; Zeiss, Oberkochen, Germany). Excitation lines of 488 and 568 nm were used to detect Alexa 488 (BP 505- to 550-nm emission) and LysoTracker/Cy3 fluorescence (LP585 emission), respectively. Optical sections were set at <1  $\mu$ m.

### Statistical Analysis

Values are expressed as means ± SE. Statistical significance was evaluated using one-way ANOVA, followed by Fisher's multiple-range test. Differences were considered significant at  $P < 0.05$ .

## RESULTS

### Plasma Appearance of Denatured Albumins in Oxidative Stress in Vivo

In this study, we first attempted to confirm whether denatured albumins such as those we previously identified in rats

with endotoxigenesis generally increase in response to other kinds of oxidative stress. For this purpose, we used five kinds of oxidative stress: IHD, diabetes, acute inflammation, endotoxigenesis, and aging. As shown in Table 1, plasma TBARS levels were significantly higher (2.5 to 4.0 fold) in the five models of oxidative stress compared with young control rats, and severe hypoalbuminemia was observed in IHD, acute inflammation, and endotoxigenesis. Accordingly, a negative correlation ( $R = -0.94$ ) between plasma TBARS levels and plasma concentrations of total albumin was observed (see Fig. 2A). We next determined the presence of denatured albumins using the purified IgG against the specific epitopes of M-Alb. Two major immunoreactive plasma albumins were detected at the same  $R_f$  values as those of D2 (0.39) and D3 (0.26) albumin in rats with endotoxigenesis on PVDF membrane transferred from native PAGE gels (Fig. 1A). The  $\alpha$ -helical content of D2-like and D3-like albumin was 32–33% and –4–0%, respectively, and there was no significant difference among the five models. Lysosomal enzymes isolated from rat liver were used to estimate the proteolytic susceptibility of these albumins. The percentage of the original band remaining on PVDF membrane transferred from SDS-PAGE gels at 2 h after incubation with lysosomal enzymes was 54–61% in D2-like albumin and 31–36% in D3-like albumin. Again, we observed no significant differences in proteolytic susceptibility of these albumins in response to each treatment. On the basis of the results described above, we confirmed that D2 and D3 albumins are generally recognized in the oxidative stress used in this study.

Plasma concentrations of D2 and D3 albumin increased significantly in the five kinds of oxidative stress (Fig. 1, B and C). The increments in D2 and D3 albumin, however, were not necessarily the same when compared under the same oxidative stress. Figure 2, B and C, shows the correlation between plasma TBARS levels and plasma concentrations of D2 and D3 albumin. A positive correlation ( $R = 0.87$ ) was observed between plasma levels of TBARS and D3 albumin. Altogether, two kinds of denatured (D2 and D3) albumin are generally

Table 1. Plasma thiobarbituric acid-reactive substance, plasma total albumin, and body weight in the five kinds of oxidative stress

Subjects	TBARS, nmol/ml	Total Albumin, mg/ml	Body Wt, g
Control, 7 wk	0.42 ± 0.07	50.6 ± 4.3	253.3 ± 2.3
IHD	1.67 ± 0.14‡	25.3 ± 4.3‡	235.3 ± 6.4*
Diabetes	1.12 ± 0.10‡	35.6 ± 3.7*	222.3 ± 5.5‡
Acute inflammation	1.61 ± 0.15‡	17.6 ± 9.2‡	211.1 ± 3.2‡
Endotoxigenesis	1.63 ± 0.19‡	27.0 ± 4.0*	213.2 ± 6.0‡
Aging, 6 mo	1.03 ± 0.14‡	43.2 ± 0.2	526.0 ± 17.2‡

Values are means ± SE of data from three rats. *N*<sup>o</sup>-nitro-L-arginine methyl ester (L-NAME), streptozotocin (STZ), turpentine oil, and lipopolysaccharide (LPS) were administered to induce ischemic heart disease (IHD), diabetes, acute inflammation, and endotoxigenesis, respectively. Blood samples were obtained at the most severe period in each treatment used in this study: IHD at 10 days, diabetes at 7 days, acute inflammation at 2 days, and endotoxigenesis at 1.5 days after the injection. Six-month-old rats were used for aged rats without any treatment. Plasma thiobarbituric acid-reactive substance (TBARS) levels were determined fluorometrically (59), and total albumin was determined using anti-rat albumin antibody. Statistical significance was evaluated using one-way ANOVA followed by Fisher's multiple-range tests. \* $P < 0.05$ , † $P < 0.01$ , and ‡ $P < 0.001$  vs. control.

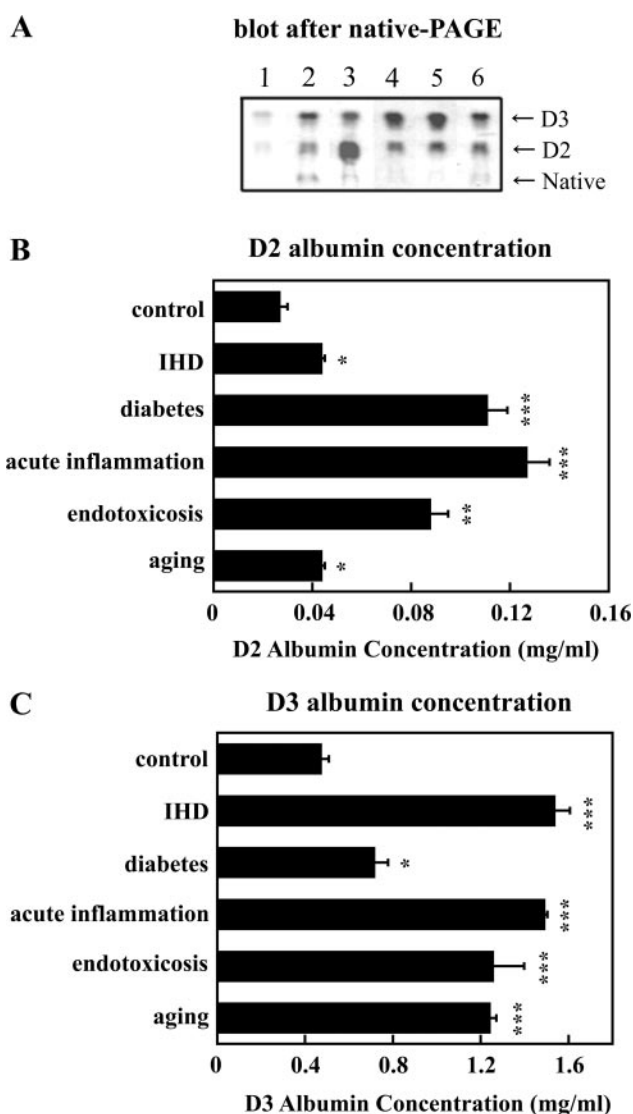


Fig. 1. Plasma concentrations of denatured albumin in rats under five kinds of oxidative stress. Rat plasma was sampled from control and five kinds of oxidative stress [ischemic heart disease (IHD), diabetes, acute inflammation, endotoxigenesis, and aging] and was subjected to native PAGE and transferred onto polyvinylidene difluoride (PVDF) membrane. Purified IgG against the specific epitope of maleylated albumin (M-Alb) was used to detect denatured (D2 and D3) albumins on the membrane. A: Western blot profile; lane 1, control; lane 2, IHD; lane 3, diabetes; lane 4, acute inflammation; lane 5, endotoxigenesis; and lane 6, aging. The fluorescence intensity was quantified using the FluorImager 595. B and C: D2 and D3 albumin concentrations, respectively. Blood samples were collected at the most severe period of individual stress (see Table 1). Values are means ± SE of three rats. Statistical significance was evaluated using one-way ANOVA followed by Fisher's multiple range test. \* $P < 0.05$ , \*\* $P < 0.01$ , and \*\*\* $P < 0.001$  vs. control.

recognized, and their plasma concentrations increase in response to the oxidative stress used in this study.

#### Binding Characteristics of D3 Albumin to Liver Membrane Proteins

To characterize the binding properties of D3 albumin to liver membrane proteins, ligand blot analysis with several competitors was performed. FITC-labeled D3 albumin (30  $\mu$ g/ml each) bound to the 18- and 30-kDa proteins on the PVDF

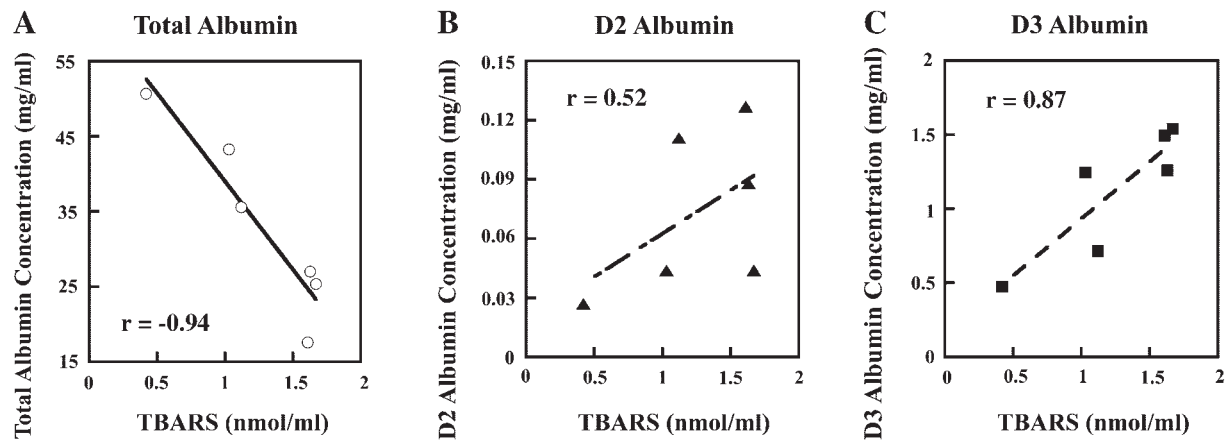


Fig. 2. Relationships between plasma levels of thiobarbituric acid-reactive substance (TBARS) and albumins. Total albumin (native + denatured,  $\circ$ ), D2 ( $\blacktriangle$ ), and D3 albumins ( $\blacksquare$ ) were quantified using native PAGE followed by Western blot analysis (see Table 1 and Fig. 1). Plasma TBARS levels were quantified using a fluorescence spectrophotometer (see Table 1). A–C: relationships for total, D2, and D3 albumins, respectively.

membrane (Fig. 3A, lane 1). FITC-labeled chemically modified albumins, M-Alb and F-Alb (30  $\mu\text{g/ml}$  each), bound similarly to the 18- and 30-kDa proteins on the PVDF membrane. The same concentration (30  $\mu\text{g/ml}$ ) of FITC-labeled native albumin showed no detectable bands against liver membrane proteins (Fig. 3A, lane 2). However, FITC-labeled native albumin bound to 18-, 30-, and 60-kDa proteins at the higher concentration of 3 mg/ml (Fig. 3A, lane 3). On the basis of the molecular weights and their binding characteristics to several albumins, we judged these 18- and 30-kDa proteins to be gp18 and gp30, respectively, both of which were previously reported by Schnitzer and colleagues (47, 51). The 60-kDa protein is thought to be gp60, which is known as the receptor for transcytosis of native albumin in endothelial cells (32, 49, 57, 58).

Further binding characteristics of D3 albumin to gp18 and gp30 membrane proteins are shown in Fig. 3, B and C. A 10-fold excess of unlabeled F-Alb, M-Alb, and D3 albumin significantly reduced the FITC-labeled D3 albumin binding to <20%. Anti-gp18 IgG, anti-gp30 IgG, and specific M-Alb IgG reduced the binding to <40%, respectively. Furthermore, polyanionic macromolecules (dextran sulfate, fucoidan), and concanavalin A reduced the binding to <50%. On the other hand, native albumin and preimmune IgG were not the competitors for FITC-labeled D3 albumin binding. These results indicate that both gp18 and gp30 recognize D3 albumin as well as M-Alb and F-Alb and that ionic (electrostatic) interactions participate in the binding.

#### Kinetic Analysis of the Cellular Binding, Uptake, and Degradation of D3 Albumin

LECs in culture were used to assess the binding, uptake, and degradation of D3 albumin. The total binding of FITC-labeled D3 albumin to LECs increased up to the maximum dose (3  $\mu\text{g/ml}$ ) we used. However, the specific binding, which can be calculated by subtracting the nonspecific binding from the total binding, showed a saturable curve (Fig. 4A). Figure 4B shows the Scatchard plot of the specific binding, which gave parameters of  $K_d = 1.9 \mu\text{g/ml}$  and  $B_{\text{max}} = 102.5 \text{ ng/mg}$  of cell protein. We next examined the uptake of D3 albumin by LECs. The specific uptake of D3 albumin increased in a dose-dependent manner (Fig. 4C) and exhibited a maximal ligand uptake

of 551 ng/mg of cell protein. Degradation of FITC-labeled D3 albumin estimated on the basis of the acid-soluble intensities of fluorescence increased similarly to the uptake (Fig. 4D). Approximately one-fifth of the fluorescence was observed in the acid-soluble fraction compared with the uptake at the end of the 2-h incubation.

FITC-labeled F-Alb (but not D3 albumin) showed similar characteristics of binding, uptake, and degradation by LECs. FITC-labeled native albumin, however, showed negligible binding, uptake, and degradation compared with D3 albumin and F-Alb (data not shown).

#### Effects of Antibodies and Polyanionic Molecules on the Cellular Binding, Uptake, and Degradation of D3 Albumin

To evaluate the quantitative significance of gp18 and gp30 on the cellular binding, uptake, and degradation of D3 albumin, LECs were incubated with FITC-labeled D3 albumin and anti-gp18 IgG, anti-gp30 IgG, equimolar mixtures of gp18 and gp30 IgG, specific M-Alb IgG, and polyanionic molecules. A 10-fold molar excess of anti-gp18 IgG and anti-gp30 IgG reduced the binding of FITC-labeled D3 albumin to LECs to  $\sim 70\%$  and  $\sim 60\%$  of preimmune IgG, respectively (Fig. 5). The equimolar mixture of the IgG showed an additive inhibitory effect on the binding, resulting in  $\sim 20\%$  of the binding of the preimmune IgG. A 10-fold molar excess of specific M-Alb IgG reduced the binding to  $\sim 10\%$  of preimmune IgG. Polyanionic molecules, the same as those described in *Binding characteristics of D3 albumin to liver membrane proteins*, and for concanavalin A, reduced the binding to 20–70% of preimmune IgG, depending on the kinds of molecules (dextran sulfate and fucoidan are shown in Fig. 5). F-Alb and D3 albumin reduced the binding of FITC-labeled D3 albumin to LECs to  $\sim 10\%$  of preimmune IgG. Native albumin did not significantly reduce the binding. Similar results were observed regarding the uptake of D3 albumin.

Further analyses of the IgG regarding the specific uptake and degradation of D3 albumin were performed using increasing concentrations of the IgG. An inhibitory effect of the anti-gp18 IgG on the uptake of D3 albumin reached a plateau value (70–80% of the control) at a concentration of  $\sim 20 \mu\text{g/ml}$ , and the effect did not change up to 100  $\mu\text{g/ml}$  (Fig. 6A). The same

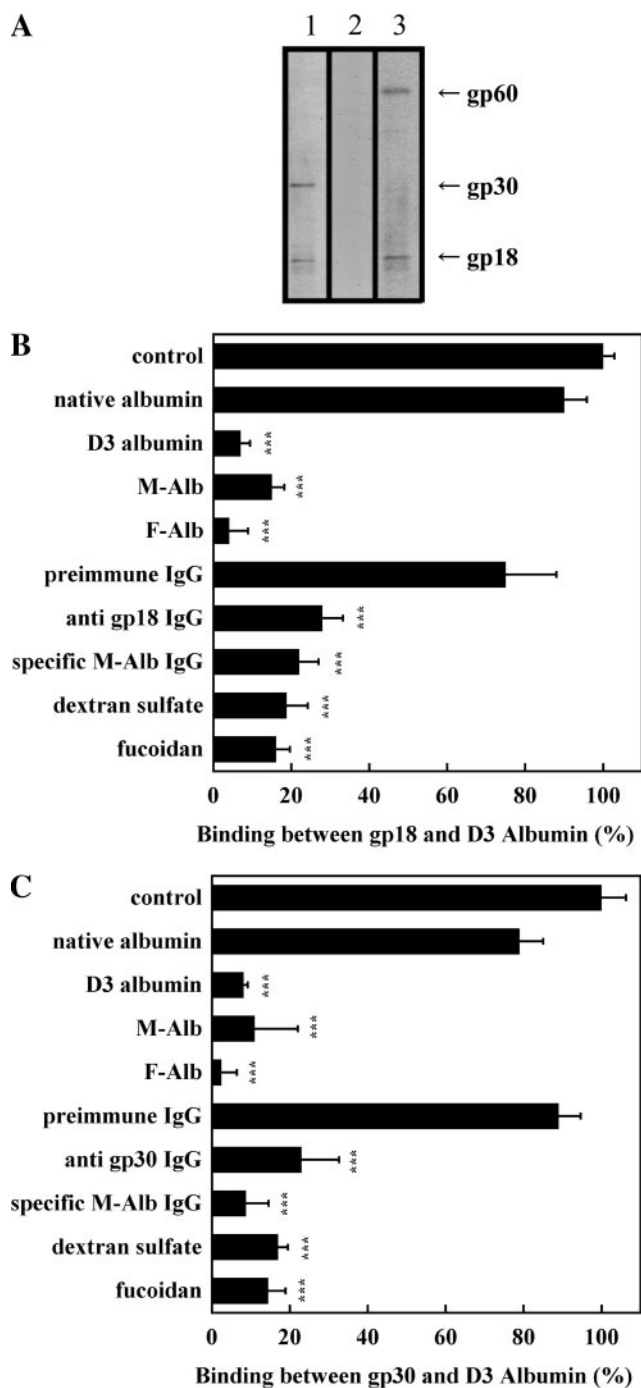


Fig. 3. Competitive analysis of D3 albumin binding to gp18 and gp30. Liver membrane proteins were separated by performing SDS-PAGE and transferred onto a PVDF membrane filter. The binding of fluorescein isothiocyanate (FITC)-labeled D3 albumin was estimated in the presence of a 10-fold molar excess of proteins and 1 mg/ml polyanionic molecules indicated in the ordinate. Specific M-Alb IgG refers to the purified IgG against the specific epitopes of M-Alb. The fluorescence intensities of the bands were determined using the FluorImager 595. *A*: profile of the binding of the FITC-labeled D3 albumin (lane 1; 30  $\mu$ g/ml) and FITC-labeled native albumin (lane 2, 30  $\mu$ g; lane 3, 3 mg/ml) to liver membrane proteins without competitors. *B* and *C*: inhibition of FITC-labeled D3 albumin binding to gp18 and gp30 by the indicated competitors, respectively. Values are means  $\pm$  SE of four observations. Statistical significance was evaluated using one-way ANOVA followed by Fisher's multiple-range test. \*\*\* $P < 0.001$  vs. control.

but a slightly stronger inhibitory effect was observed when anti-gp30 IgG was used. The equimolar mixture of both anti-gp18 and anti-gp30 IgG showed additive inhibitory effects on the uptake of D3 albumin, resulting in  $\sim 20\%$  of the control value at a concentration of 20  $\mu$ g/ml and up to 100  $\mu$ g/ml. The specific M-Alb IgG inhibited the uptake of D3 albumin most effectively, resulting in  $\sim 10\%$  of the control at a concentration of 20  $\mu$ g/ml and up to 100  $\mu$ g/ml. Similar inhibitory effects of IgG were observed in the degradation of D3 albumin (Fig. 6B). These results support the data shown in Figs. 3 and 5 and suggest that gp18 and gp30 are the main receptors for D3 albumin degradation in LECs.

Laser-scanning confocal microscopy was used to confirm the results obtained above. LECs were incubated with Lyso-Tracker (a red fluorescent marker of the acidic lysosomal compartment) and Alexa 488-labeled D3 albumin for 2 h at 37°C. An overlay plot of these color distributions within the cell demonstrated that most of the D3 albumin existed in the lysosome (Fig. 7A). The localization of cell surface gp18 and the binding site of D3 albumin were confirmed using an unsaturable dose (3  $\mu$ g/ml) of Cy3-labeled anti-gp18 IgG and Alexa 488-labeled D3 albumin. Again, these two colors coexisted on the cell surface (Fig. 7B). Confocal images of Cy3-labeled anti-gp30 IgG were similar to those of Cy3-labeled anti-gp18 IgG (data not shown). A saturable dose (100  $\mu$ g/ml) of the equimolar mixture of anti-gp18 and anti-gp30 IgG completely blocked the D3 albumin binding (Fig. 7C). Altogether, we confirmed that D3 albumin binds primarily to the cell surface proteins, gp18 and gp30, and is degraded in the lysosome of LECs.

*Endocytic Pathways for D3 Albumin Degradation*

We next attempted to elucidate the endocytic pathway of D3 albumin in LECs. For this purpose, we used two kinds of inhibitors: PAO (an inhibitor of clathrin-related endocytosis) as well as filipin and digitonin (inhibitors of caveolae-related endocytosis). PAO had no significant effects on the uptake and degradation of D3 albumin during the incubation for 2 h at 37°C. In contrast, both filipin and digitonin showed a strong inhibitory effect on the uptake and degradation of D3 albumin, resulting in reduced uptake and degradation to  $\sim 20\%$  of the control (Fig. 8). These results indicate that D3 albumin is degraded in the lysosome via caveolae-related endocytosis after binding to the cell surface receptors, gp18 and gp30. Confocal microscopic observations support the data shown in Fig. 8. Intracellular D3 albumin (green in Fig. 9B) coexisted with the lysosome in the presence of PAO, but no fluorescent signals derived from D3 albumin were observed in the presence of filipin (Fig. 9A).

**DISCUSSION**

The major findings of the present study are as follows: 1) plasma concentrations of denatured (D2 and D3) albumin increase in response to oxidative stress, 2) D3 albumin binds to gp18 and gp30 membrane proteins prepared from rat liver, 3) gp18- and gp30-mediated endocytosis is the primary pathway for the degradation of D3 albumin in LECs, and 4) D3 albumin is incorporated into LECs by caveolae-related endocytosis and reaches the lysosome. We discuss these points in order below.

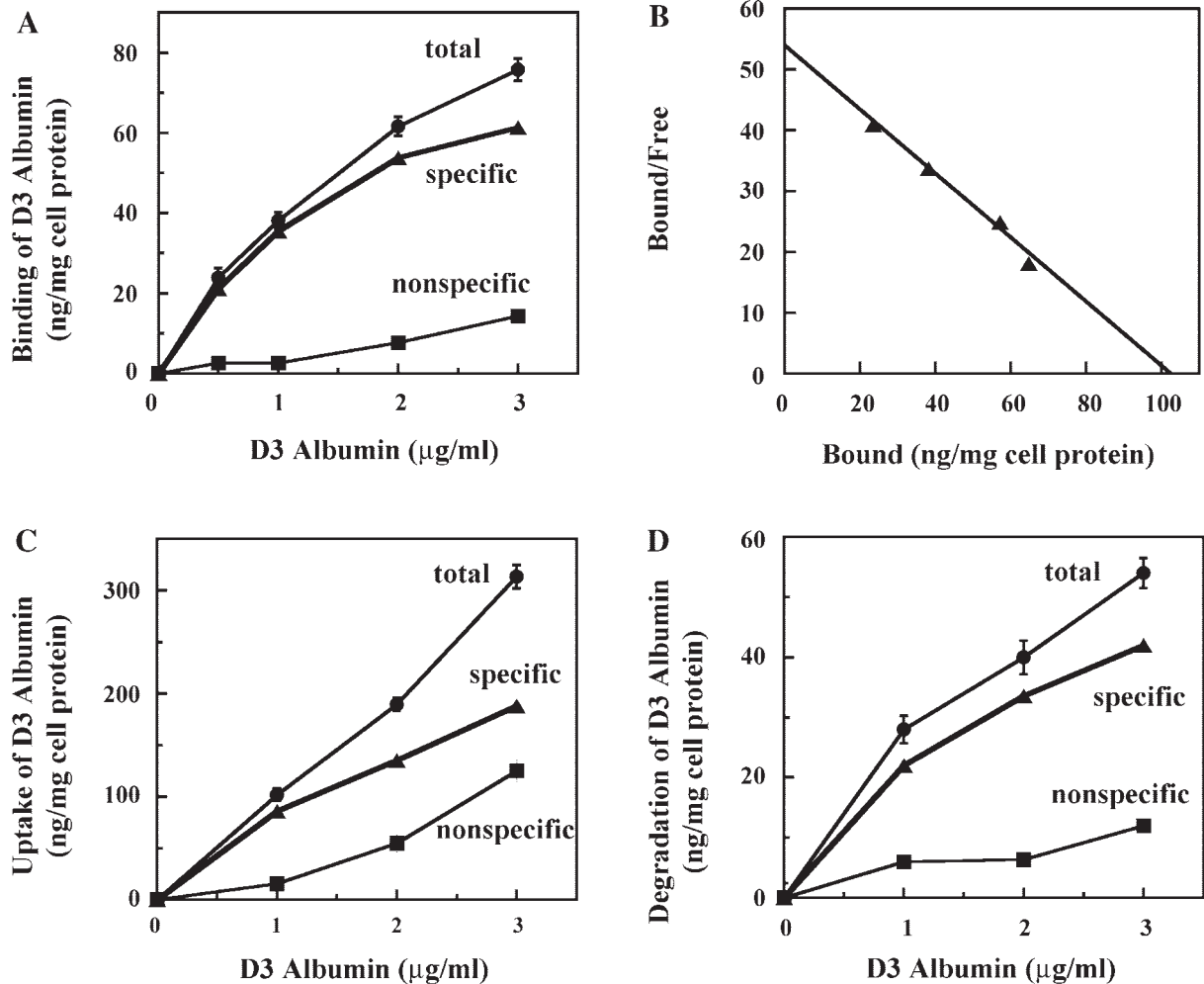


Fig. 4. Kinetics of the cellular binding, uptake, and degradation of D3 albumin. *A*: cellular binding kinetics of FITC-labeled D3 albumin were investigated in primary cultured liver endothelial cells (LECs) incubated at 4°C for 2 h. The nonspecific binding was determined in the presence of unlabeled D3 albumin (20-fold excess), and the specific binding was calculated by subtracting the nonspecific binding from the total binding. *B*: Scatchard plot of the specific binding curve shown in *A*. *C*: cellular uptake of D3 albumin was analyzed in the same manner as in the binding analysis, except for an incubation temperature of 37°C. *D*: cellular degradation of D3 albumin was estimated from the intensities of acid-soluble fluorescence in the cellular fraction. LECs were incubated in the same manner used for cellular uptake. Values are means  $\pm$  SE of three observations.

#### Oxidative Stress and Plasma Concentrations of Denatured Albumins

We used five models of oxidative stress, including IHD, diabetes, acute inflammation, endotoxemia, and aging. First, we determined the plasma levels of TBARS and total albumin in these five models to confirm whether the rats were under oxidative stress. As shown in Table 1, we observed an increased level of TBARS in all models of oxidative stress used in this study, and these results are consistent with previous reports regarding IHD (10), diabetes (30), inflammation (8), and aging (24). Meanwhile, total albumin decreased, which also has been reported previously for IHD (14), diabetes (19), acute inflammation (52), endotoxemia (4), and aging (41). In the present study, we observed a negative correlation between plasma TBARS and total albumin in the five models of oxidative stress, and the correlation coefficient was  $-0.94$  through the models. These results suggest that the rats were under oxidative stress, although the severity of the oxidative stress differed within the models. We next determined the plasma

concentrations of denatured (D2 and D3) albumin, both of which were previously isolated in rats with endotoxemia (4), and found that levels of both D2 and D3 albumin increased significantly in the five models of oxidative stress (Figs. 1 and 2). Plasma levels of D3 albumin showed a positive correlation with that of TBARS ( $R = 0.87$ ). These results may indicate that free radical species attack plasma albumin and that the denatured albumins caused by the reaction are rapidly eliminated from the circulating blood, resulting in subsequently decreased concentrations of total albumin.

Plasma albumin is known to be a labile molecule against oxidative damage. It is thought to act as an antioxidant in the body to protect against oxidation of body components such as low-density lipoproteins (15) and bound fatty acids (42). Kaski et al. (53) reported that IHD increases levels of ischemia modified albumin, which has no ability to bind cobalt. Era and colleagues have reported that diabetes (54) and aging (16) result in increased levels of oxidized albumin (nonmercaptalbumin). It is also known that albumin is denatured by free radicals in vitro (12).

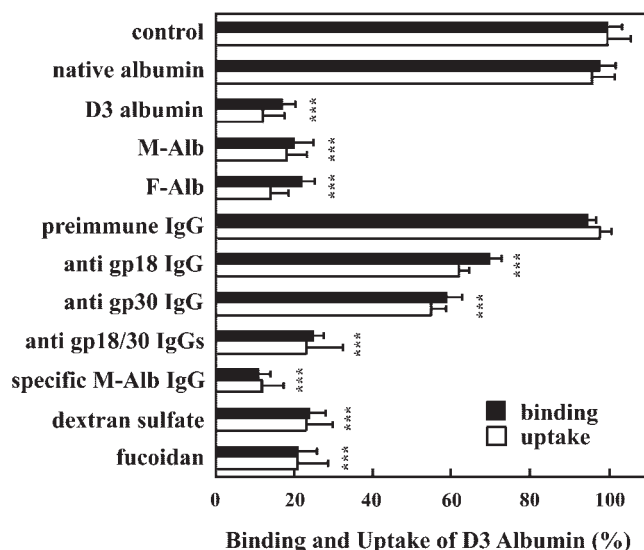


Fig. 5. Inhibition of cellular binding and uptake of D3 albumin by anti-gp18 IgG, anti-gp30 IgG, specific M-Alb IgG, and polyanionic molecules. LECs were incubated with FITC-labeled D3 albumin and a 10-fold molar excess of the molecules indicated in the ordinate for 2 h. Anti-gp18/anti-gp30 IgG refers to the equimolar mixture of anti-gp18 IgG and anti-gp30 IgG. Specific M-Alb IgG refers to the purified IgG against the specific epitopes of M-Alb. Binding (closed bar) and uptake (open bar) were performed at 4°C and 37°C, respectively. After being washed with PBS, the cellular intensities of fluorescence were determined using the FluorImager 595. Data are expressed as a percentage of the signal observed in the control. Values are means  $\pm$  SE of three observations. Statistical significance was evaluated using one-way ANOVA followed by Fisher's multiple-range tests. \*\*\* $P < 0.001$  vs. control.

As described above, many kinds of modified and structurally altered albumins, including D2 and D3 albumins (4), have been reported. However, little is known about their degradative nature on a molecular basis. We therefore next attempted to characterize the degradative process of D3 albumin by using primary cultured rat liver endothelial cells.

#### D3 Albumin Binding to gp18 and gp30 Membrane Proteins

In previous studies by Schnitzer and colleagues (47, 51), chemically denatured albumin such as F-Alb has been found to bind the 18- and 30-kDa proteins referred to as gp18 and gp30 from rat liver. In the present study, we attempted to confirm whether these membrane proteins equally recognize physiologically denatured albumin, D3 albumin. By using chemically modified albumins (F-Alb, M-Alb) and IgG against gp18 and gp30, the binding nature of D3 albumin to gp18 and gp30 was investigated using ligand blot analysis. A 10-fold molar excess of unlabeled D3 albumin significantly reduced the binding of FITC-labeled D3 albumin to gp18 and gp30 (Fig. 3, B and C). The same effects were observed when FITC-labeled D3 albumin competed with F- and M-Alb, but not with native albumin. These results suggest that D3 albumin, F-Alb, and M-Alb expose the common binding sites to gp18 and gp30, which are hidden inside the molecule in the native state. This exposure may enable these three denatured albumins to compete with the binding to gp18 and gp30 membrane proteins.

Antibody against the specific epitopes of M-Alb as well as anti-gp18 and anti-gp30 IgG inhibited the D3 albumin binding to gp18 and gp30 membrane proteins to a similar degree (Fig. 3). These findings indicate that the antibodies we prepared in

this study specifically recognize the respective antigens and inhibit the binding of D3 albumin. The specific M-Alb IgG is thought to recognize D3 albumin's binding sites to gp18 and gp30 and/or to another site hidden inside the molecule in the native state.

Polyanionic molecules were used to characterize the binding between D3 albumin and gp18 or gp30. As shown in Fig. 3, dextran sulfate and fucoidan significantly inhibited the binding, suggesting that ionic (electrostatic) interactions based on charged amino acids participate in the binding. The same inhibitory effects of polyanionic molecules have been observed in the binding between chemically modified albumin and gp18 or gp30 (47) as well as in the binding of the other scavenger receptors and their respective ligands (27, 28).

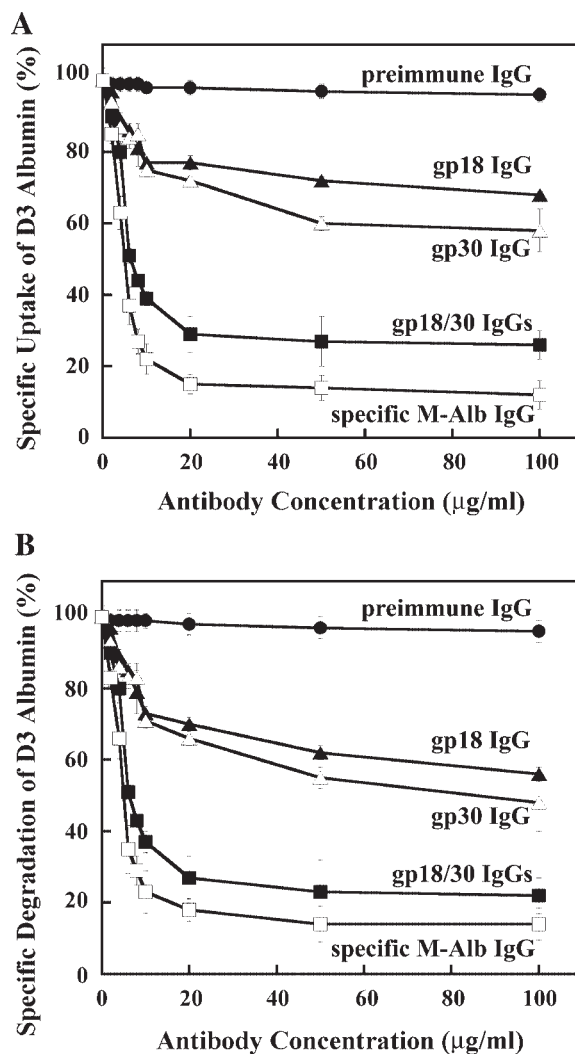


Fig. 6. Dose-dependent inhibition of cellular uptake and degradation of D3 albumin by anti-gp18 IgG, anti-gp30 IgG, and specific M-Alb IgG. LECs were incubated with FITC-labeled D3 albumin and increasing concentrations of preimmune IgG (●), anti-gp18 IgG (▲), anti-gp30 IgG (△), an equimolar mixture of these IgG (■), or specific M-Alb IgG (□; purified IgG against specific epitopes of M-Alb) for 2 h at 37°C, respectively. Cellular uptake of D3 albumin was evaluated as the total intensities of cellular fluorescence, and degradation was evaluated as the acid-soluble intensities of cellular fluorescence. Data are expressed as a percentage of the signal observed in the control. A: cellular uptake of D3 albumin. B: degradation of D3 albumin. Values are means  $\pm$  SE of three observations.

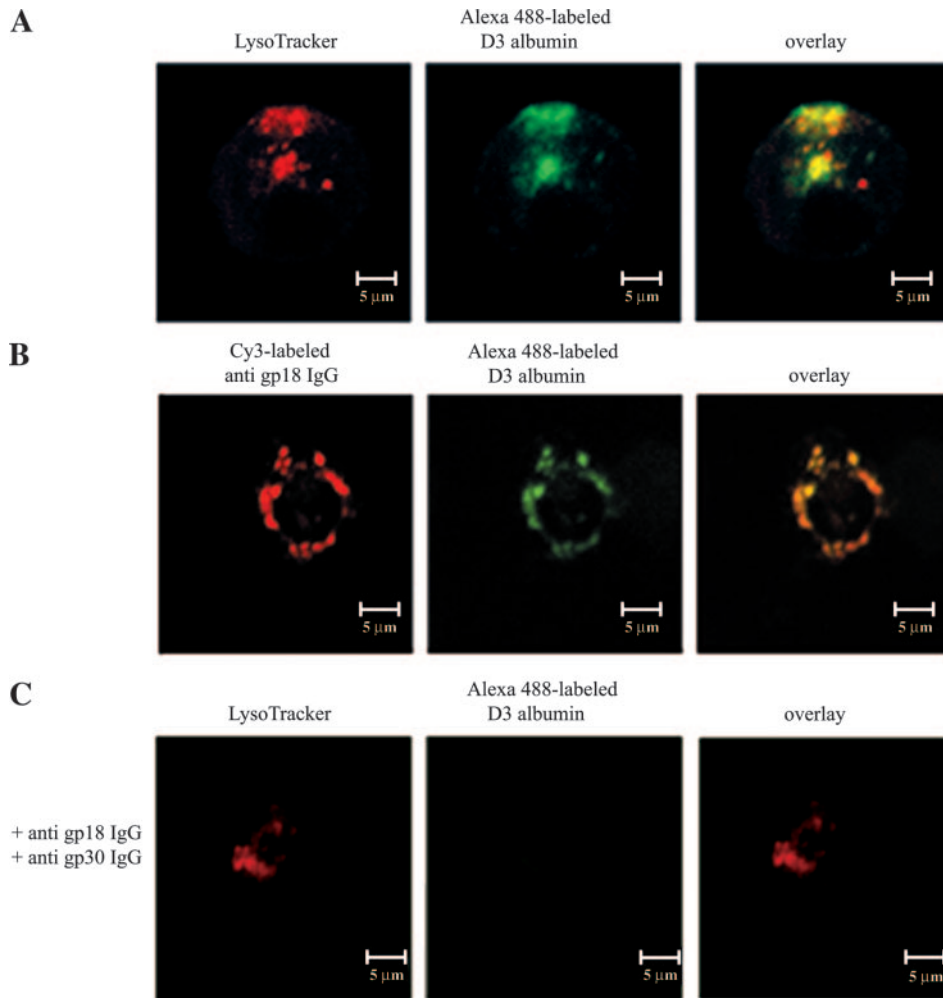


Fig. 7. Confocal microscopic observations of LECs. LECs were incubated for 2 h at 37°C (A and C) or 4°C (B) with Alexa 488-labeled D3 albumin (green) and the indicated compounds. *A*: intracellular distributions of LysoTracker (a red fluorescent marker of the lysosomal compartment) and D3 albumin (green). The overlay plot (yellow) of these two colors indicates that D3 albumin existed in the lysosome within the LECs. *B*: cell surface distribution of gp18 and the binding sites of D3 albumin. Cy3-labeled anti-gp18 IgG (3 µg/ml; red) and Alexa 488-labeled D3 albumin (green) were added to the medium and incubated for 2 h at 4°C. The same distribution patterns between gp18 and D3 albumin were observed on the cell surface. *C*: inhibitory effects of anti-gp18 and anti-gp30 IgG on the incorporation of D3 albumin into LECs. The same condition used in *A* was used, except for the addition of anti-gp18 and anti-gp30 IgG. The equimolar mixture of these IgG (100 µg/ml) completely blocked the incorporation of D3 albumin. Each image is typical of three experiments in different cultures. Scale bar, 5 µm.

Many signal sequences such as PEST, KFERQ, YXRF, NPXY, COOH-terminal dileucine motif (LL), and so forth have been reported (6, 13). The binding motif of albumin molecules to gp18 and gp30 receptors is of great interest with regard to albumin degradation, because this sequence could possibly recognize the albumin molecule to be broken down in the circulating blood. This sequence has not yet been elucidated, however, because the precise characteristics of gp18 and gp30, including their cDNA sequences, have not been investigated.

#### Binding, Uptake, and Degradation of D3 Albumin by LECs in Culture

Kinetic analysis of D3 albumin binding to LECs was performed (Fig. 4A). A Scatchard plot of the specific binding (Fig. 4B) revealed the following cell-protein parameters:  $K_d = 1.9$  µg/ml (28.6 nM) and  $B_{max} = 102.5$  ng/mg. The binding affinity of D3 albumin to LECs is thought to be high compared with values reported previously in the literature; that is, the affinity between M-Alb and the microvascular endothelial cells from the epididymal fat pad ( $K_d = 48$  nM) (47) and the affinity between modified albumin such as AGE-BSA and LOX-1 cells ( $K_d = 149$  nM) (23) or AGE-BSA and CD36 ( $K_d = 62$  nM) (34). Such a high affinity between D3 albumin and LECs may contribute to the rapid elimination of denatured albumin from

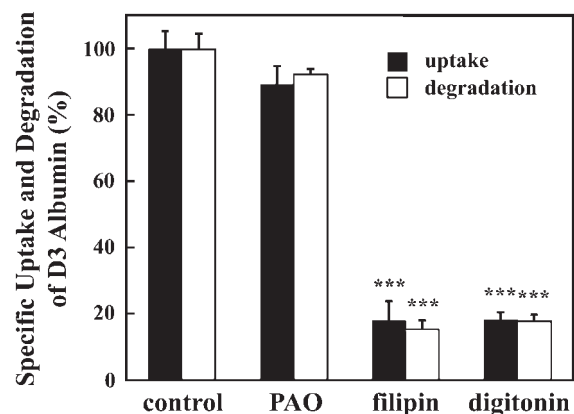


Fig. 8. Effects of the endocytic inhibitors on the uptake and degradation of D3 albumin. LECs were incubated for 2 h at 37°C with FITC-labeled D3 albumin in the presence of phenylarsine oxide (PAO, an inhibitor of clathrin-related endocytosis), filipin, and digitonin (inhibitors of caveolae-related endocytosis). PAO (2 µM) showed no effect on the uptake and degradation of D3 albumin. In contrast, both filipin (5 µg/ml) and digitonin (4 µM) inhibited the uptake and degradation of D3 albumin to ~20% of the control level. The specific uptake (closed bar) and degradation (open bar) were estimated in the same manner as described in Fig. 4. Data are expressed as a percentage of the signal in the absence of any inhibitor (control). Statistical significance was evaluated using one-way ANOVA followed by Fisher's multiple range tests. \*\*\* $P < 0.001$  vs. control.

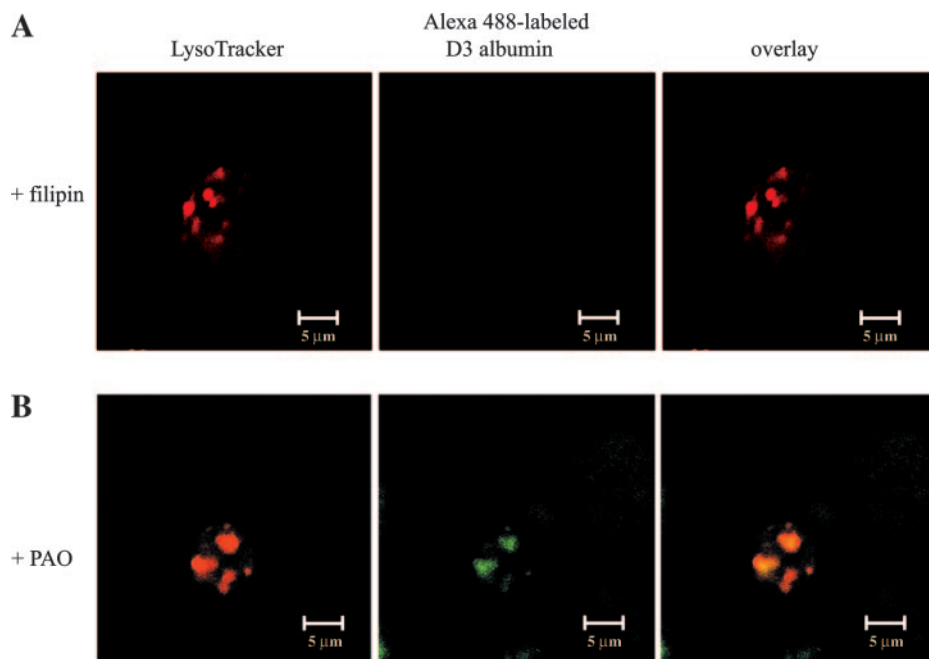


Fig. 9. Effects of endocytic inhibitors on the uptake of D3 albumin. Confocal microscopic observations of LECs. LECs were incubated for 2 h at 37°C with Alexa 488-labeled D3 albumin (green) and LysoTracker (red fluorescent marker of the lysosomal compartment) in the presence of PAO (an inhibitor of clathrin-related endocytosis) (A) or filipin (an inhibitor of caveolae-related endocytosis) (B). Each image is typical of three experiments in different cultures. Scale bar, 5 μm.

circulating blood via the endothelial cell surface receptors gp18 and gp30.

The cellular binding and uptake of FITC-labeled D3 albumin were significantly inhibited by denatured albumins (D3 albumin, F-Alb, and M-Alb) and by antibodies (against gp18, gp30, and specific epitopes of M-Alb) (Fig. 5). The same inhibitory results were observed in the ligand blot experiments (Fig. 3, B and C). The most remarkable observations regarding Figs. 5 and 6 are that anti-gp18 and gp30 IgG additively inhibited the binding and uptake of D3 albumin, resulting in an ~80% inhibition of the uptake and degradation of D3 albumin. These phenomena led us to think that gp18 and gp30 equally participate in the incorporation and degradation of D3 albumin and that most of the D3 albumin is incorporated into the cell by these receptors. The LECs degrade most of the modified albumin in the body (5). Consequently, it may be that the degradation of D3 albumin via gp18 and gp30 is the primary degradation pathway in the body. In our experiments, gp18 and gp30 shared the ability to incorporate D3 albumin into the cell. This finding may be interpreted as follows. First, gp18 and gp30 may recognize the same binding site in denatured albumin. As such, gp18 and gp30 may contribute to the degradation of denatured albumin, depending on the number and affinity of each receptor exposed on the cell surface. Second, gp18 and gp30 may recognize different sites of denatured albumin. Each receptor in this case may correspond to degraded, denatured albumin with different steric conformations resulting from various changes in body status. In any case, precise experiments are needed concerning the amino acid sequences that bind to gp18 and gp30.

#### *Incorporation of D3 Albumin by Caveolae-Related Endocytosis*

The mechanisms underlying receptor-mediated endocytosis are thought to be divided into two categories based on the proteins that participate in the endocytic process: clathrin-

related endocytosis and caveolae-related endocytosis (45). We used the specific inhibitors of these endocytic processes to confirm the process used in the degradation of D3 albumin. As shown in Fig. 8, both filipin and digitonin, specific inhibitors of caveolae-related endocytosis, inhibited the uptake and degradation of D3 albumin in LECs in culture. In contrast, PAO, an inhibitor of clathrin-related endocytosis, showed no significant effect on the uptake and degradation of D3 albumin. This evidence strongly suggests that D3 albumin travels with caveolae to the lysosome after attaching to the cell surface receptors gp18 and gp30. Confocal microscopic observations support the above hypothesis (Fig. 9). To date, the caveolin molecule has been revealed to participate in cellular trafficking of modified albumins in endothelial cells (46, 50). However, a recent report by Hansen et al. (20) indicated that endothelial cells incorporate the modified albumin using clathrin rather than caveolin vesicles. The reason for this different pathway is thought to be the difference in the albumin molecules. Intracellular transport of albumin molecules seems to take different pathways, depending on the receptors that can recognize the structural and modification nature of the albumin molecule, and this difference is partly defined as follows. Complexes with native albumin and gp60 (albondin) (32, 46, 57) and complexes with gold-albumin and gp18 and/or gp30 (46, 50) are internalized via caveolae-related endocytosis, whereas complexes of AGE-albumin and stabilin-2 (FEEL-2) are internalized via clathrin-related endocytosis (20). No data are available, however, to elucidate the cellular events occurring after albumin attaches to gp18 and gp30. In the present study, we have obtained direct evidence that physiologically denatured albumin is degraded via caveolae-mediated endocytosis after attaching to the cell surface receptors gp18 and gp30.

In summary, we first demonstrated that oxidative stress generally increases levels of denatured albumin (D2 and D3 albumin) in circulating blood in rats. Second, we have shown that D3 albumin binds to the 18- and 30-kDa membrane

proteins that have been reported as scavenger receptors named gp18 and gp30 for chemically modified albumin. Third, we have demonstrated that gp18- and gp30-mediated endocytosis is the primary pathway for the degradation of denatured albumin in primary cultured endothelial cells. Fourth, we have obtained direct evidence that caveolae-mediated endocytosis is the route for the degradation of physiologically denatured albumin after attaching to the cell-surface receptors gp18 and gp30. On the basis of these results and our previous findings, we think that we can provide a sequencing image for the degradation of serum albumin, taking into account both the generation of denatured albumin in vivo and the recognition of denatured albumin on the cell surface and intracellular events for the degradation of denatured albumin. At present, however, we have no information available that would allow us to answer the following questions. 1) Is there a receptor that can recognize native albumin and lead to its degradation? 2) Are there amino acid sequences in albumin molecules that can be recognized by gp18 and gp30? 3) What is the production rate of denatured albumin in vivo? On the basis of our present findings, we may be able to elucidate more precisely the details of the degradative process, particularly in the setting of oxidative stress.

#### ACKNOWLEDGMENTS

We thank Tatsumi Shikano and Takanori Tsugane for performing preliminary experiments and Masato Tanaka, Kouji Yashima, Toshihiro Ito, Masaaki Ozawa, and Hideo Inatomi for helpful suggestions.

#### GRANTS

This study was supported by the Research Foundation of the Institute of Science and Technology, Meiji University.

#### REFERENCES

- Adachi H, Tsujimoto M, Arai H, and Inoue K. Expression cloning of a novel scavenger receptor from human endothelial cells. *J Biol Chem* 272: 31217–31220, 1997.
- Antohe F, Heltianu C, and Simionescu M. Albumin-binding proteins of endothelial cells: immunocytochemical detection of the 18 kDa peptide. *Eur J Cell Biol* 56: 34–42, 1991.
- Bates SR, Tao JQ, Schaller S, Fisher AB, and Shuman H. Lamellar body membrane turnover is stimulated by secretagogues. *Am J Physiol Lung Cell Mol Physiol* 278: L443–L452, 2000.
- Bito R, Shikano T, and Kawabata H. Isolation and characterization of denatured serum albumin from rats with endotoxemia. *Biochim Biophys Acta* 1646: 100–111, 2003.
- Blomhoff R, Eskild W, and Berg T. Endocytosis of formaldehyde-treated serum albumin via scavenger pathway in liver endothelial cells. *Biochem J* 218: 81–86, 1984.
- Brown D. Targeting of membrane transporters in renal epithelia: when cell biology meets physiology. *Am J Physiol Renal Physiol* 278: F192–F201, 2000.
- Butler PJ, Harris JI, Hartley BS, and Leberman R. The use of maleic anhydride for the reversible blocking of amino groups in polypeptide chains. *Biochem J* 112: 679–689, 1969.
- Canali R, Vignolini F, Nobili F, and Mengheri E. Reduction of oxidative stress and cytokine-induced neutrophil chemoattractant (CINC) expression by red wine polyphenols in zinc deficiency induced intestinal damage of rat. *Free Radic Biol Med* 28: 1661–1670, 2000.
- Carter DC and Ho JX. Structure of serum albumin. *Adv Protein Chem* 45: 153–203, 1994.
- Chan SS, Monteiro HP, Deucher GP, Abud RL, Abuchalla D, and Junqueira VB. Functional activity of blood polymorphonuclear leukocytes as an oxidative stress biomarker in human subjects. *Free Radic Biol Med* 24: 1411–1418, 1998.
- Chen YH, Yang JT, and Martinez HM. Determination of the secondary structures of proteins by circular dichroism and optical rotatory dispersion. *Biochemistry* 11: 4120–4131, 1972.
- Davies KJ and Delsignore ME. Protein damage and degradation by oxygen radicals. III. modification of secondary and tertiary structure. *J Biol Chem* 262: 9908–9913, 1987.
- Dice JF. Molecular determinants of protein half-lives in eukaryotic cells. *FASEB J* 1: 349–357, 1987.
- Djoussé L, Rothman KJ, Cupples LA, Arnett DK, and Ellison RC. Relation between serum albumin and carotid atherosclerosis: the NHLBI Family Heart Study. *Stroke* 34: 53–57, 2003.
- Dobrian A, Mora R, Simionescu M, and Simionescu N. In vitro formation of oxidatively-modified and reassembled human low-density lipoproteins: antioxidant effect of albumin. *Biochim Biophys Acta* 1169: 12–24, 1993.
- Era S, Kuwata K, Imai H, Nakamura K, Hayashi T, and Sogami M. Age-related change in redox state of human serum albumin. *Biochim Biophys Acta* 1247: 12–16, 1995.
- Fields R. The measurement of amino groups in proteins and peptides. *Biochem J* 124: 581–590, 1971.
- Gekle M, Freudinger R, and Mildenerberger S. Inhibition of Na<sup>+</sup>-H<sup>+</sup> exchanger-3 interferes with apical receptor-mediated endocytosis via vesicle fusion. *J Physiol* 531: 619–629, 2001.
- Greive KA, Osicka TM, Russo LM, and Comper WD. Nephrotic-like proteinuria in experimental diabetes. *Am J Nephrol* 23: 38–46, 2003.
- Hansen B, Longati P, Elvevold K, Nedredal GI, Schledzewski K, Olsen R, Falkowski M, Kzhyskowska J, Carlsson F, Johansson S, Smedsrød B, Goerdt S, Johansson S, and McCourt P. Stabilin-1 and stabilin-2 are both directed into the early endocytic pathway in hepatic sinusoidal endothelium via interactions with clathrin/AP-2, independent of ligand binding. *Exp Cell Res* 303: 160–173, 2005.
- Horiuchi S, Takata K, and Morino Y. Characterization of a membrane-associated receptor from rat sinusoidal liver cells that binds formaldehyde-treated serum albumin. *J Biol Chem* 260: 475–481, 1985.
- John TA, Vogel SM, Minshall RD, Ridge K, Tirupathi C, and Malik AB. Evidence for the role of alveolar epithelial gp60 in active transalveolar albumin transport in the rat lung. *J Physiol* 533: 547–559, 2001.
- Jono T, Miyazaki A, Nagai R, Sawamura T, Kitamura T, and Horiuchi S. Lectin-like oxidized low density lipoprotein receptor-1 (LOX-1) serves as an endothelial receptor for advanced glycation end products (AGE). *FEBS Lett* 511: 170–174, 2002.
- Junqueira VB, Barros SB, Chan SS, Rodrigues L, Giavarotti L, Abud RL, and Deucher GP. Aging and oxidative stress. *Mol Aspects Med* 25: 5–16, 2004.
- Kataoka C, Egashira K, Ishibashi M, Inoue S, Ni W, Hiasa K, Kitamoto S, Usui M, and Takeshita A. Novel anti-inflammatory actions of amlodipine in a rat model of arteriosclerosis induced by long-term inhibition of nitric oxide synthesis. *Am J Physiol Heart Circ Physiol* 286: H768–H774, 2004.
- Khan MA, Kumar Y, and Tayyab S. Bilirubin binding properties of pigeon serum albumin and its comparison with human serum albumin. *Int J Biol Macromol* 30: 171–178, 2002.
- Kodama T, Freeman M, Rohrer L, Zabrecky J, Matsudaira P, and Krieger M. Type I macrophage scavenger receptor contains alpha-helical and collagen-like coiled coils. *Nature* 343: 531–535, 1990.
- Kodama T, Reddy P, Kishimoto C, and Krieger M. Purification and characterization of a bovine acetyl low density lipoprotein receptor. *Proc Natl Acad Sci USA* 85: 9238–9242, 1988.
- Li YM, Mitsuhashi T, Wojciechowicz D, Shimizu N, Li J, Stitt A, He C, Banerjee D, and Vlassara H. Molecular identity and cellular distribution of advanced glycation end product receptors: relationship of p60 to OST-48 and p90 to 80K-H membrane proteins. *Proc Natl Acad Sci USA* 93: 11047–11052, 1996.
- Mahesh T and Menon VP. Quercetin alleviates oxidative stress in streptozotocin-induced diabetic rats. *Phytother Res* 18: 123–127, 2004.
- Mego JL. Role of thiols, pH and cathepsin D in the lysosomal catabolism of serum albumin. *Biochem J* 218: 775–783, 1984.
- Minshall RD, Tirupathi C, Vogel SM, and Malik AB. Vesicle formation and trafficking in endothelial cells and regulation of endothelial barrier function. *Histochem Cell Biol* 117: 105–112, 2002.
- Neeper M, Schmidt AM, Brett J, Yan SD, Wang F, Pan YC, Elliston K, Stern RD, and Shaw A. Cloning and expression of a cell surface receptor for advanced glycosylation end products of proteins. *J Biol Chem* 267: 14998–15004, 1992.
- Ohgami N, Nagai R, Ikemoto M, Arai H, Kuniyasu A, Horiuchi S, and Nakayama H. Cd36, a member of the class b scavenger receptor family,

- as a receptor for advanced glycation end products. *J Biol Chem* 276: 3195–3202, 2001.
35. Ohgami N, Nagai R, Miyazaki A, Ikemoto M, Arai H, Horiuchi S, and Nakayama H. Scavenger receptor class B type I-mediated reverse cholesterol transport is inhibited by advanced glycation end products. *J Biol Chem* 276: 13348–13355, 2001.
  36. Ohshita T and Kido H. Simple preparation of rat brain lysosomes and their proteolytic properties. *Anal Biochem* 230: 41–47, 1995.
  37. Ohshita T, Kominami E, Ii K, and Katunuma N. Effect of starvation and refeeding on autophagy and heterophagy in rat liver. *J Biochem (Tokyo)* 100: 623–632, 1986.
  38. Ottnad E, Via DP, Frubis J, Sinn H, Friedrich E, Ziegler R, and Dresel HA. Differentiation of binding sites on reconstituted hepatic scavenger receptors using oxidized low-density lipoprotein. *Biochem J* 281: 745–751, 1992.
  39. Ottnad E, Via DP, Sinn H, Friedrich E, Ziegler R, and Dresel HA. Binding characteristics of reduced hepatic receptors for acetylated low-density lipoprotein and maleylated bovine serum albumin. *Biochem J* 265: 689–698, 1990.
  40. Panés J, Kurose I, Rodriguez-Vaca D, Anderson DC, Miyasaka M, Tso P, and Granger DN. Diabetes exacerbates inflammatory responses to ischemia-reperfusion. *Circulation* 93: 161–167, 1996.
  41. Peters T Jr. *All About Albumin: Biochemistry, Genetics, and Medical Applications*. San Diego, CA: Academic, 1996.
  42. Radi R, Bush KM, Cosgrove TP, and Freeman BA. Reaction of xanthine oxidase-derived oxidants with lipid and protein of human plasma. *Arch Biochem Biophys* 286: 117–125, 1991.
  43. Sawamura T, Kume N, Aoyama T, Moriwaki H, Hoshikawa H, Aiba Y, Tanaka T, Miwa S, Katsura Y, Kita T, and Masaki T. An endothelial receptor for oxidized low-density lipoprotein. *Nature* 386: 73–77, 1997.
  44. Schmidt AM, Vianna M, Gerlach M, Brett J, Ryan J, Kao J, Esposito C, Hegarty H, Hurley W, and Clauss M. Isolation and characterization of two binding proteins for advanced glycosylation end products from bovine lung which are present on the endothelial cell surface. *J Biol Chem* 267: 14987–14997, 1992.
  45. Schnitzer JE. Caveolae: from basic trafficking mechanisms to targeting transcytosis for tissue-specific drug and gene delivery in vivo. *Adv Drug Delivery Res* 49: 265–280, 2001.
  46. Schnitzer JE, Allard J, and Oh P. NEM inhibits transcytosis, endocytosis, and capillary permeability: implication of caveolae fusion in endothelia. *Am J Physiol Heart Circ Physiol* 268: H48–H55, 1995.
  47. Schnitzer JE and Bravo J. High affinity binding, endocytosis, and degradation of conformationally modified albumins: potential role of gp30 and gp18 as novel scavenger receptors. *J Biol Chem* 268: 7562–7570, 1993.
  48. Schnitzer JE, Carley WW, and Palade GE. Albumin interacts specifically with a 60-kDa microvascular endothelial glycoprotein. *Proc Natl Acad Sci USA* 85: 6773–6777, 1988.
  49. Schnitzer JE and Oh P. Albondin-mediated capillary permeability to albumin: differential role of receptors in endothelial transcytosis and endocytosis of native and modified albumins. *J Biol Chem* 269: 6072–6082, 1994.
  50. Schnitzer JE, Oh P, Pinney E, and Allard J. Filipin-sensitive caveolae-mediated transport in endothelium: reduced transcytosis, scavenger endocytosis, and capillary permeability of select macromolecules. *J Cell Biol* 127: 1217–1232, 1994.
  51. Schnitzer JE, Sung A, Horvat R, and Bravo J. Preferential interaction of albumin-binding proteins, gp30 and gp18, with conformationally modified albumins. *J Biol Chem* 267: 24544–24553, 1992.
  52. Schreiber G, Howlett G, Nagashima M, Millership A, Martin H, Urban J, and Kotler L. The acute phase response of plasma protein synthesis during experimental inflammation. *J Biol Chem* 257: 10271–10277, 1982.
  53. Sinha MK, Gaze DC, Tippins JR, Collinson PO, and Kaski JC. Ischemia modified albumin is a sensitive marker of myocardial ischemia after percutaneous coronary intervention. *Circulation* 107: 2403–2405, 2003.
  54. Suzuki E, Yasuda K, Takeda N, Sakata S, Era S, Kuwata K, Sogami M, and Miura K. Increased oxidized form of human serum albumin in patients with diabetes mellitus. *Diabetes Res Clin Pract* 18: 153–158, 1992.
  55. Tamura Y, Adachi H, Osuga J, Ohashi K, Yahagi N, Sekiya M, Okazaki H, Tomita S, Iizuka Y, Shimano H, Nagai R, Kimura S, Tsujimoto M, and Ishibashi S. FEEL-1 and FEEL-2 are endocytic receptors for advanced glycation end products. *J Biol Chem* 278: 12613–12617, 2003.
  56. Tiruppathi C, Finnegan A, and Malik AB. Isolation and characterization of a cell surface albumin-binding protein from vascular endothelial cells. *Proc Natl Acad Sci USA* 93: 250–254, 1996.
  57. Tiruppathi C, Song W, Bergenfeldt M, Sass P, and Malik AB. Gp60 activation mediates albumin transcytosis in endothelial cells by tyrosine kinase-dependent pathway. *J Biol Chem* 272: 25968–25975, 1997.
  58. Vogel SM, Easington CR, Minshall RD, Niles WD, Tiruppathi C, Hollenberg SM, Parrillo JE, and Malik AB. Evidence of transcellular permeability pathway in microvessels. *Microvasc Res* 61: 87–101, 2001.
  59. Yagi K. Assay for blood plasma or serum. *Methods Enzymol* 105: 328–331, 1984.
  60. Yamane A, Seetharam L, Yamaguchi S, Gotoh N, Takahashi T, Neufeld G, and Shibuya M. A new communication system between hepatocytes and sinusoidal endothelial cells in liver through vascular endothelial growth factor and Flt tyrosine kinase receptor family (Flt-1 and KDR/Flk-1). *Oncogene* 9: 2683–2690, 1994.